LOW-COMPLEXITY AND HIGH-ACCURACY ODD-ORDER VARIABLE FRACTIONAL-DELAY DIGITAL FILTERS

Tian-Bo Deng

Department of Information Science
Faculty of Science, Toho University
Miyama 2-2-1, Funabashi, Chiba 274-8510, Japan
E-mail: deng@is.sci.toho-u.ac.jp

ABSTRACT

This paper presents a new minimax method for designing low-complexity and high-accuracy odd-order finite-impulse-response (FIR) variable fractional-delay (VFD) digital filters. The objective of the minimax design is to minimize the maximum absolute error of the variable frequency response (VFR) by utilizing the second-order cone programming (SOCP) and achieves a global minimax solution. We formulate the SOCP minimax design by using different-order sub-filters in the Farrow structure such that the complexity of an odd-order FIR VFD filter can be reduced. An odd-order design example is given to demonstrate the effectiveness of the new SOCP-based minimax design approach.

Index Terms— Variable digital filter, variable fractional-delay (VFD), odd-order FIR VFD digital filter, second-order cone programming (SOCP), minimax design.

1. INTRODUCTION

The digital filters with changeable frequency responses are referred to as *variable digital filters*. Applying variable digital filters during signal processing does not necessitate redesigning a new filter, and a new frequency response can be easily obtained. Basically, variable filters include those with variable magnitude responses [1]-[5] or/and variable fractional-delay (VFD) responses [6]-[18]. Without redesigning a new filter, the users can instantly tune the frequency response of a variable digital filter on-line. VFD filters have found various signal processing applications such as sampling rate conversion [6], discrete-time signal interpolations [7], and fractional-order differentiator design [8].

The main objective of this paper is to formulate the minimax design of an odd-order finite-impulse-response (FIR) VFD filter as a second-order cone programming (SOCP) problem that can be efficiently solved by using a primal-dual interior-point method. The SOCP has been successfully utilized to design even-order VFD filters [17], which guarantees the optimality of the minimax solution in the sense that the maximum absolute VFR error is truly minimized, i.e., the minimax design is an exact solution without any approximation. Since the SOCP-based minimax design uses different-order sub-filters in the Farrow structure, we also apply a one-by-one increase scheme to simultaneously optimize all the sub-filter orders such that a given maximum design error bound is exactly met. This reduces the total VFD filter complexity and yields an optimal low-complexity structure. An odd-order design example is given to demonstrate the effectiveness of the SOCP design formulation.

2. VFR ERROR OF ODD-ORDER VFD FILTER

This section first derives the VFR error using the transfer function with different-order sub-filters, which is necessary for formulating the SOCP-based minimax design to be stated in the next section.

The ideal VFR of an odd-order FIR VFD filter is

$$H_{\rm I}(\omega, d) = e^{-j\omega d} \tag{1}$$

where $\omega \in [0, \alpha\pi]$, and d is the VFD parameter, $d \in [0, 1]$. In order to exploit the coefficient symmetry proved in [11] in the minimax design, we substitute

$$d = \frac{1}{2} + p, \quad p \in [-0.5, 0.5]$$

and yield

$$H_{\rm I}(\omega, d) = e^{-j\frac{\omega}{2}} \hat{H}_{\rm I}(\omega, p) \tag{2}$$

with

$$\hat{H}_{\rm I}(\omega, p) = e^{-j\omega p}. \tag{3}$$

To approximate (2), we use the transfer function

$$H(z, p) = \sum_{n=-N}^{N+1} h_n(p) z^{-n} \tag{4}$$

with variable coefficients

$$h_n(p) = \sum_{m=0}^{M} a(n, m) p^m. \tag{5}$$

Substituting (5) into (4) leads to

$$\begin{aligned} H(z, p) &= \sum_{n=-N}^{N+1} \sum_{m=0}^{M} a(n, m) z^{-n} p^m \\ &= \sum_{m=0}^{M} \left[\sum_{n=-N}^{N+1} a(n, m) z^{-n} \right] p^m \\ &= \sum_{m=0}^{M_{\rm e}} F_m(z) p^{2m} + \sum_{m=1}^{M_{\rm o}} G_m(z) p^{2m-1} \end{aligned} \tag{6}$$

where $M_{\rm e}$, $M_{\rm o}$ are defined as

$$M_{\rm e} = \left\lfloor \frac{M}{2} \right\rfloor, \quad M_{\rm o} = \left\lceil \frac{M}{2} \right\rceil \tag{7}$$

$\lfloor\ \rfloor$, $\lceil\ \rceil$ are floor and ceiling functions, respectively, and

$$
\begin{aligned}
F_m(z) &= \sum_{n=-N}^{N+1} a(n, 2m) z^{-n} \\
G_m(z) &= \sum_{n=-N}^{N+1} a(n, 2m-1) z^{-n}
\end{aligned}
\tag{8}
$$

are odd-order sub-filters in the Farrow structure. Fig. 1 illustrates an example of the Farrow structure with $(M_e, M_o) = (1, 2)$. As we have proved in [11], the coefficient symmetry

$$
a(1-n, m) = (-1)^m \cdot a(n, m) \tag{9}
$$

holds, i.e., the sub-filters $F_m(z)$ have even-symmetric coefficients, and $G_m(z)$ have odd-symmetric (anti-symmetric) coefficients. Substituting (9) into (8) yields

$$
\begin{aligned}
F_m(z) &= z^{-\frac{1}{2}} \hat{F}_m(z) \\
G_m(z) &= z^{-\frac{1}{2}} \hat{G}_m(z)
\end{aligned}
$$

with

$$
\begin{aligned}
\hat{F}_m(z) &= \sum_{n=1}^{N+1} a(n, 2m) \left[z^{(n-\frac{1}{2})} + z^{-(n-\frac{1}{2})} \right] \\
\hat{G}_m(z) &= -\sum_{n=1}^{N+1} a(n, 2m-1) \left[z^{(n-\frac{1}{2})} - z^{-(n-\frac{1}{2})} \right].
\end{aligned}
$$

Hence, the transfer function (6) can be rewritten as

$$
H(z, p) = z^{-\frac{1}{2}} \hat{H}(z, p) \tag{10}
$$

with

$$
\hat{H}(z, p) = \sum_{m=0}^{M_e} \hat{F}_m(z) p^{2m} + \sum_{m=1}^{M_o} \hat{G}_m(z) p^{2m-1}. \tag{11}
$$

Comparing (2) with (10) shows that $\hat{H}(z, p)$ approximates $\hat{H}_I(\omega, p)$ in (3). Here, $\hat{F}_m(z)$ and $\hat{G}_m(z)$ may take different orders. Using different-order sub-filters obtains the frequency responses of $\hat{F}_m(z)$ and $\hat{G}_m(z)$ as

$$
\begin{aligned}
\hat{F}_m(\omega) &= \sum_{n=1}^{N_{em}+1} b_{em}(n) \cos(n - \frac{1}{2})\omega = \mathbf{c}_m^T \mathbf{b}_{em} \\
\hat{G}_m(\omega) &= (-j) \cdot \sum_{n=1}^{N_{om}+1} b_{om}(n) \sin(n - \frac{1}{2})\omega \\
&= (-j) \cdot \mathbf{s}_m^T \mathbf{b}_{om}
\end{aligned}
\tag{12}
$$

where

$$
\begin{aligned}
b_{em}(n) &= 2a(n, 2m), \qquad n = 1, 2, \cdots, (N_{em}+1) \\
b_{om}(n) &= 2a(n, 2m-1), \quad n = 1, 2, \cdots, (N_{om}+1)
\end{aligned}
\tag{13}
$$

$$
\begin{aligned}
\mathbf{c}_m^T &= \begin{bmatrix} \cos(\frac{\omega}{2}) & \cos(\frac{3\omega}{2}) & \cdots & \cos(N_{em} + \frac{1}{2})\omega \end{bmatrix} \\
\mathbf{s}_m^T &= \begin{bmatrix} \sin(\frac{\omega}{2}) & \sin(\frac{3\omega}{2}) & \cdots & \sin(N_{om} + \frac{1}{2})\omega \end{bmatrix}
\end{aligned}
$$

and

$$
\mathbf{b}_{em} = \begin{bmatrix} b_{em}(1) \\ b_{em}(2) \\ \vdots \\ b_{em}(N_{em}+1) \end{bmatrix}, \quad \mathbf{b}_{om} = \begin{bmatrix} b_{om}(1) \\ b_{om}(2) \\ \vdots \\ b_{om}(N_{om}+1) \end{bmatrix}
$$

are coefficient vectors of $F_m(z)$ and $G_m(z)$ as shown in (13). Consequently, the frequency response of $\hat{H}(z, p)$ becomes

$$
\begin{aligned}
\hat{H}(\omega, p) &= \sum_{m=0}^{M_e} \left(\mathbf{c}_m^T \mathbf{b}_{em} \right) p^{2m} - j \sum_{m=1}^{M_o} \left(\mathbf{s}_m^T \mathbf{b}_{om} \right) p^{2m-1} \\
&= \sum_{m=0}^{M_e} \mathbf{f}_m^T \mathbf{b}_{em} - j \sum_{m=1}^{M_o} \mathbf{g}_m^T \mathbf{b}_{om} \\
&= \mathbf{f}^T \mathbf{b}_e - j \mathbf{g}^T \mathbf{b}_o
\end{aligned}
\tag{14}
$$

where

$$
\begin{aligned}
\mathbf{f}_m^T &= p^{2m} \mathbf{c}_m^T, \qquad \mathbf{f}^T = \begin{bmatrix} \mathbf{f}_0^T & \mathbf{f}_1^T & \cdots & \mathbf{f}_{M_e}^T \end{bmatrix} \\
\mathbf{g}_m^T &= p^{2m-1} \mathbf{s}_m^T, \quad \mathbf{g}^T = \begin{bmatrix} \mathbf{g}_1^T & \mathbf{g}_1^T & \cdots & \mathbf{g}_{M_o}^T \end{bmatrix}
\end{aligned}
$$

$$
\mathbf{b}_e = \begin{bmatrix} \mathbf{b}_{e0} \\ \mathbf{b}_{e1} \\ \vdots \\ \mathbf{b}_{eM_e} \end{bmatrix}, \quad \mathbf{b}_o = \begin{bmatrix} \mathbf{b}_{o1} \\ \mathbf{b}_{o2} \\ \vdots \\ \mathbf{b}_{oM_o} \end{bmatrix}. \tag{15}
$$

Thus, the VFR error between $\hat{H}(\omega, p)$ and $\hat{H}_I(\omega, p)$ is

$$
\begin{aligned}
\hat{e}(\omega, p) &= \hat{H}(\omega, p) - \hat{H}_I(\omega, p) \\
&= e_R(\omega, p) - j e_I(\omega, p)
\end{aligned}
\tag{16}
$$

with

$$
\begin{aligned}
e_R(\omega, p) &= \mathbf{f}^T \mathbf{b}_e - \cos(\omega p) \\
e_I(\omega, p) &= \mathbf{g}^T \mathbf{b}_o - \sin(\omega p).
\end{aligned}
\tag{17}
$$

3. ODD-ORDER SOCP DESIGN FORMULATION

The minimax design can be formulated as

$$
\begin{aligned}
&\text{minimize} \quad \epsilon \\
&\text{subject to} \quad |\hat{e}(\omega, p)| \le \epsilon
\end{aligned}
\tag{18}
$$

with

$$
|\hat{e}(\omega, p)| = \sqrt{e_R^2(\omega, p) + e_I^2(\omega, p)} \tag{19}
$$

i.e., the coefficient vectors $\mathbf{b}_e$ and $\mathbf{b}_o$ in (15) can be simultaneously optimized by solving the SOCP problem

$$
\begin{aligned}
&\text{minimize} \quad \epsilon \\
&\text{subject to} \quad \sqrt{e_R^2(\omega, p) + e_I^2(\omega, p)}| \le \epsilon
\end{aligned}
\tag{20}
$$

where the constraint is quadratic (conic), i.e., the vector

$$
\begin{bmatrix} \epsilon \\ e_R(\omega, p) \\ e_I(\omega, p) \end{bmatrix} = \begin{bmatrix} \epsilon \\ -\cos(\omega p) + \mathbf{f}^T \mathbf{b}_e \\ -\sin(\omega p) + \mathbf{g}^T \mathbf{b}_o \end{bmatrix} \in \mathcal{K}_q \tag{21}
$$

where $\mathcal{K}_q$ is called quadratic cone or second-order cone (SOC), and the vector in (21) is affine in ϵ, $\mathbf{b}_\mathrm{e}$, and $\mathbf{b}_\mathrm{o}$. Let

$$\begin{aligned}\mathbf{y} &= \begin{bmatrix}\epsilon & \mathbf{b}_\mathrm{e}^T & \mathbf{b}_\mathrm{o}^T\end{bmatrix}^T \\ \mathbf{b}^T &= \begin{bmatrix}-1 & 0 & \cdots & 0\end{bmatrix}\end{aligned} \tag{22}$$

the minimax design (20) can be formulated as the SOCP problem (dual SOCP problem)

$$\begin{aligned}&\text{maximize} \quad \mathbf{b}^T\mathbf{y} \\ &\text{subject to} \quad \mathbf{c} - \mathbf{A}^T\mathbf{y} \in \mathcal{K}_q\end{aligned} \tag{23}$$

where

$$\mathbf{c} = \begin{bmatrix}0 \\ -\cos(\omega p) \\ -\sin(\omega p)\end{bmatrix}, \quad \mathbf{A}^T = -\begin{bmatrix}1 & \mathbf{0} & \mathbf{0} \\ 0 & \mathbf{f}^T & \mathbf{0} \\ 0 & \mathbf{0} & \mathbf{g}^T\end{bmatrix}. \tag{24}$$

Since ω and p take continuous values, the discretized version of (23) can be solved on a set of discrete points (ω_{l_1}, p_{l_2}) by sampling $\omega \in [0, \alpha\pi]$ and $p \in [0, 0.5]$ with step sizes $\alpha\pi/(L_1 - 1)$ and $0.5/(L_2 - 1)$, respectively. The number of total discrete points is $L_1 L_2$. As a result, the SOCP design can be formulated as

$$\begin{aligned}&\text{maximize} \quad \mathbf{b}^T\mathbf{y} \\ &\text{subject to} \quad \mathbf{c}_l - \mathbf{A}_l^T\mathbf{y} \in \mathcal{K}_q, \quad l = 1, 2, \cdots, L\end{aligned} \tag{25}$$

where L is the total number of discrete points, $L = L_1 L_2$. The SOCP problem in (25) can be solved by using the well-known efficient software *SeDuMi*.

4. ODD-ORDER DESIGN EXAMPLE

The ideal VFR in (1) is approximated with $\alpha = 0.9$ such that the maximum VFR error is below the upper error bound -100 dB. By setting $(M_\mathrm{e}, M_\mathrm{o}) = (3, 4)$, $(L_1, L_2) = (201, 31)$, and sub-filter orders

$$\begin{aligned}\begin{bmatrix}N_{\mathrm{e}1} & N_{\mathrm{e}2} & N_{\mathrm{e}3}\end{bmatrix} &= \begin{bmatrix}33 & 32 & 24 & 12\end{bmatrix} \\ \begin{bmatrix}N_{\mathrm{o}1} & N_{\mathrm{o}2} & N_{\mathrm{o}3} & N_{\mathrm{o}4}\end{bmatrix} &= \begin{bmatrix}17 & 16 & 10 & 2\end{bmatrix}\end{aligned} \tag{26}$$

where the sub-filter orders are obtained by applying a one-by-one increase scheme that simultaneously optimizes the sub-filter orders $\begin{bmatrix}N_{\mathrm{e}1} & N_{\mathrm{e}2} & N_{\mathrm{e}3}\end{bmatrix}$ and $\begin{bmatrix}N_{\mathrm{o}1} & N_{\mathrm{o}2} & N_{\mathrm{o}3} & N_{\mathrm{o}4}\end{bmatrix}$. Thus, the total number of the VFD filter coefficients is 154.

To evaluate the design accuracy, we use the maximum VFR error in decibel (dB) defined as

$$\epsilon_\mathrm{Max} = \max\left\{20\log_{10}|\hat{e}(\omega, p)|, \omega \in [0, \alpha\pi], p \in [-0.5, 0.5]\right\} \tag{27}$$

and the normalized root-mean-square (NRMS) VFR error

$$\epsilon_2 = \left[\frac{\displaystyle\int_0^{\alpha\pi}\int_{-0.5}^{0.5}|\hat{e}(\omega, p)|^2 dp d\omega}{\displaystyle\int_0^{\alpha\pi}\int_{-0.5}^{0.5}|\hat{H}_\mathrm{I}(\omega, p)|^2 dp d\omega}\right]^{1/2} \times 100\%. \tag{28}$$

Both the above two errors are numerically evaluated by discretizing $\omega \in [0, \alpha\pi]$ with step size $\alpha\pi/200$ and $p \in [-0.5, 0.5]$ with step size $1/60$, which generates 201 points for $\omega \in [0, \alpha\pi]$ and 61 points for $p \in [-0.5, 0.5]$. The design errors are

$$\epsilon_\mathrm{Max} = -100.09 \text{ (dB)}, \quad \epsilon_2 = 0.000702\%. \tag{29}$$

If the decoupling linear programming (LP) technique is used [18], which linearizes the non-linear minimax design as two separate LP designs, the number of total VFD filter parameters is 159 in order to satisfy the upper error bound, and the resulting design errors are

$$\epsilon_\mathrm{Max} = -100.24 \text{ (dB)}, \quad \epsilon_2 = 0.000562\%. \tag{30}$$

Therefore, the SOCP design requires fewer paramters (4 parameters less) than the LP technique to meet the given upper error bound -100 dB, but its NRMS error becomes slightly larger. Theoretically, the SOCP design yields the global minimax solution, while the decoupling LP design is somewhat simpler but only yields an approximate minimax solution. Therefore, there is a trade-off between the design accuracy and the design computation. As long as the slightly increased computation required in the design is affordable, the SOCP technique may be preferable because it always generate the globally optimal minimax design.

Fig. 2 depicts the absolute VFR errors from the odd-order SOCP design. Obviously, all the VFR errors are below -100 dB. Fig. 3 shows the VFD response, and Fig. 4 plots its absolute errors with maximum value 0.000719.

5. CONCLUSION

This paper has formulated a global minimax method for designing an odd-order FIR VFD digital filter with different-order sub-filters. The minimax design is achieved by using the SOCP, which is a more general convex programming than the LP and theoretically yields the optimal minimax solution. By using both the SOCP formulation and different-order sub-filters, an odd-order low-complexity and high-accuracy VFD filter can be designed. A design example has been given to illustrate the global optimality of the SOCP design and the low-complexity of the resulting odd-order VFD filter.

6. REFERENCES

[1] R. Zarour and M. M. Fahmy, “A design technique for variable digital filters”, *IEEE Trans. Circuits Syst.*, vol. 36, no. 11, pp. 1473-1478, Nov. 1989.

[2] T.-B. Deng and T. Soma, “Variable digital filter design using the outer product expansion,” *IEE Proc. Vision, Image and Signal Process.*, vol. 141, no. 2, pp. 123-128, Apr. 1994.

[3] T.-B. Deng, “Design of recursive 1-D variable filters with guaranteed stability,” *IEEE Trans. Circuits Syst. II, Analog Digit. Signal Process.*, vol. 44, no. 9, pp. 689-695, Sep. 1997.

[4] T.-B. Deng, “Weighted least-squares method for designing arbitrarily variable 1-D FIR digital filters,” *Signal Process.*, vol. 80, no. 4, pp. 597-613, Apr. 2000.

[5] J.-J. Shyu, S.-C. Pei, and Y.-D. Huang, “Design of variable two-dimensional FIR digital filters by McClellan transformation,” *IEEE Trans. Circuits Syst. I, Reg. Papers*, vol. 56, no. 3, pp. 574-582, Mar. 2009.

[6] C. W. Farrow, “A continuously variable digital delay element,” *Proc. 1988 IEEE Int. Symp. Circuits Syst.*, vol. 3, pp. 2641-2645, Espoo, Finland, Jun. 6-9, 1988.

[7] G.-S. Liu and C.-W. Wei, “A new variable fractional sample delay filter with nonlinear interpolation,” *IEEE Trans. Circuits Syst. II, Analog Digit. Signal Process.*, vol. 39, no. 2, pp. 123-126, Feb. 1992.

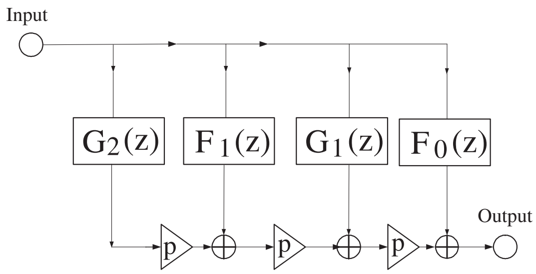

Fig. 1. Farrow structure with $(M_\mathrm{e}, M_\mathrm{o}) = (1, 2)$.

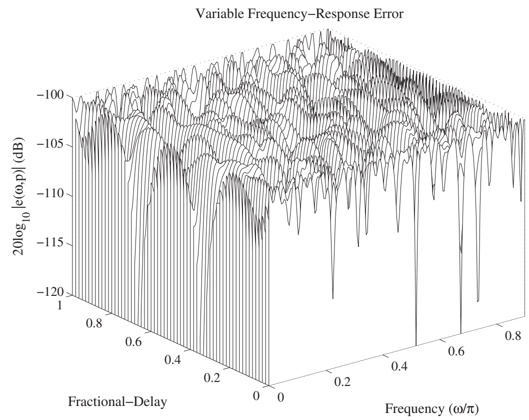

Fig. 2. Absolute VFR errors (odd-order SOCP design).

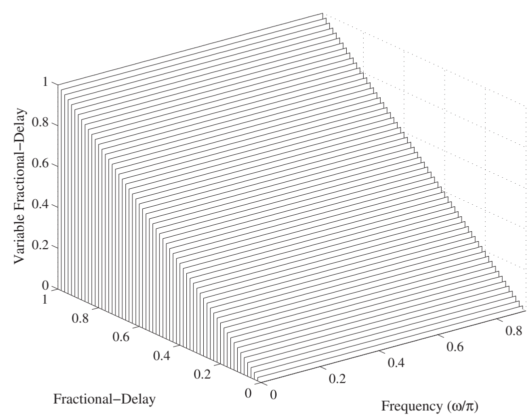

Fig. 3. VFD response (odd-order SOCP design).

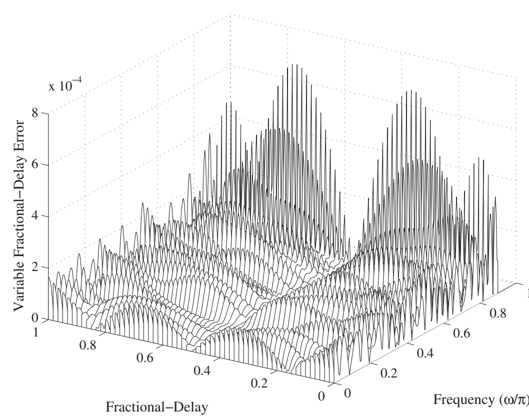

Fig. 4. Absolute VFD errors (odd-order SOCP design).

[8] C.-C. Tseng, "Improved design of digital fractional-order differentiators using fractional sample delay," *IEEE Trans. Circuits Syst. I, Reg. Papers*, vol. 53, no. 1, pp. 193-203, Jan. 2006.

[9] T.-B. Deng, "Coefficient-symmetries for implementing arbitrary-order Lagrange-type variable fractional-delay digital filters," *IEEE Trans. Signal Process.*, vol. 55, no. 8, pp. 4078-4090, Aug. 2007.

[10] T.-B. Deng, "Robust structure transformation for causal Lagrange-type variable fractional-delay filters," *IEEE Trans. Circuits Syst. I: Reg. Papers*, vol. 56, no. 8, pp. 1681-1688, Aug. 2009.

[11] T.-B. Deng, "Symmetric structures for odd-order maximally flat and weighted-least-squares variable fractional-delay filters," *IEEE Trans. Circuits Syst. I, Reg. Papers*, vol. 54, no. 12, pp. 2718-2732, Dec. 2007.

[12] T.-B. Deng and W.-S. Lu, "Weighted least-squares method for designing variable fractional delay 2-D FIR digital filters," *IEEE Trans. Circuits Syst. II Analog Digit. Signal Process.*, vol. 47, pp. 114-124, Feb. 2000.

[13] T.-B. Deng, "Discretization-free design of variable fractional-delay FIR digital filters," *IEEE Trans. Circuits Syst. II, Analog Digit. Signal Process.*, vol. 48, no. 6, pp. 637-644, Jun. 2001.

[14] T.-B. Deng, "Closed-form design and efficient implementation of variable digital filters with simultaneously tunable magnitude and fractional-delay," *IEEE Trans. Signal Process.*, vol. 52, no. 6, pp. 1668-1681, Jun. 2004.

[15] T.-B. Deng and Y. Lian, "Weighted-least-squares design of variable fractional-delay FIR filters using coefficient-symmetry," *IEEE Trans. Signal Process.*, vol. 54, no. 8, pp. 3023-3038, Aug. 2006.

[16] T.-B. Deng and Y. Nakagawa, "SVD-based design and new structures for variable fractional-delay digital filters," *IEEE Trans. Signal Process.*, vol. 52, no. 9, pp. 2513-2527, Sep. 2004.

[17] T.-B. Deng, "Minimax design of low-complexity even-order variable fractional-delay filters using second-order cone programming," *IEEE Trans. Circuits Syst. II, Exp. Briefs*, vol. 58, no. 10, pp. 692-696, Oct. 2011.

[18] T.-B. Deng, "Decoupling minimax design of low-complexity variable fractional-delay FIR digital filters," *IEEE Trans. Circuits Syst. I, Reg. Papers*, vol. 58, no. 10, pp. 2398-2408, Oct. 2011.